International Journal of Heat and Technology
Vol. 42, No. 4, August, 2024, pp. 1406-1416
Journal homepage: http://iieta.org/journals/ijht

Experimental and Numerical Investigation of PV Panel Cooling Using Ribbed Fin Heat Exchanger and Hybrid Generation

Hussein A. Idan*, Hatam K. Kadhom, Sahar R. Faraj

Electromechanical Engineering Department, University of Technology-Iraq, Baghdad 10066, Iraq

Corresponding Author Email: eme.20.02@grad.uotechnology.edu.iq

https://doi.org/10.18280/ijht.420430

Received: 15 May 2024
Revised: 26 July 2024
Accepted: 9 August 2024
Available online: 31 August 2024

Keywords:
CFD, heat transfer, heat exchanger, PVT system, solar energy, thermoelectric generator units (TEGs)

ABSTRACT

The high temperature of photovoltaic panels represents the most prominent challenge to the possibility of increasing their efficiency. To eliminate excess heat, a PVT system is used with an efficient cooling system. The current study focuses on economic and easy new construction. The main objective of this study is to provide more information about the cooling effect on performance under certain operating conditions. This study involved initial numerical testing of five prototypes used to cool PV panels in a water-based system. The best model was chosen by considering the impact of cooling box geometry, heat flux variation, and coolant flow rate variation on performance. The problem was solved numerically in a 3D model using CFD technology via ANSYS R19.2 software. As for the experimental part, it includes two sections. The first represents the manufacturing of two models, one of which represents the basic model of a cooling box with non-ribbed fins (NRFCB), while the other represents the fifth model that was chosen according to the initial numerical test, which represents a cooling box with ribbed fins (RFCB). The second section consists of adding thermoelectric units (TEGs) to take advantage of the accumulated heat instead of dispersing it. The results showed good convergence between the two tests, with a deviation rate that did not exceed 7.58%. The experimental test results indicate that the PV panel cooled according to the RFCB model achieved an improvement over the NRFCB model of 0.77% and 1.26% under a heat flux of 400 and 1035 W/m², respectively, at a water rate of 4 L/min. On the other hand, the addition of 8 TEG units achieved its highest power at 14:30, which reached 0.144 W during the day on July 15, 2023, in Kut, Iraq, with a water rate of 0.5 L/min.

1. INTRODUCTION

With the worsening global energy crisis and environmental issues, and since photovoltaic cells are considered one of the most important and environmentally friendly alternatives used, they still face many technical challenges in realistic and practical use, due to their low efficiency as a result of the heat associated with solar radiation. Therefore, work is being done on how to exploit the cooling system to produce hybrid energy through the radiation falling on the panel and the heat accompanying it at the same time. The study and analysis of a cooling system that relies on the use of water flowing through the pipes formed for the cooling system to reduce the temperature of the photovoltaic panel indicates the clear effect of changing flows on its performance compared to another without cooling [1, 2]. On the other hand, adding nanofluids to water and passing them through a small external heat exchanger connected to cooling channels mounted on the PV panel improved the panel's performance [3]. As for the effect of changing the shape of the cooling channels, the results of analytical and experimental studies indicated that the use of V-shaped channels increases the surface area of heat exchange with the cooling fluid, which increases the heat transfer from the surface of the back panel to the cooling fluid, thus improving its performance and efficiency [4-7]. Analytical studies that included studying the effect of adding triangular ribs to the cooling tubes of PV panels also showed a positive effect on the performance of that panel. The effect of changing the number and size of ribs, changing operating conditions including wind speed and ambient temperature, as well as changing the coolant entry speed on performance was studied, [8]. The effect of rib spacing (between 2 ribs (S_{rib})), height (H_{rib}) and width (W_{rib}) on heat transfer properties was studied. The results indicate that the effect of S_{rib} and H_{rib} relation to the ribbed heat sink is more effective than W_{rib}. This effect appears on the movement of fluids as a result of friction with the ribs, that increases heat dissipation [9-11].

Studying the properties of flow states numerically and analytically, especially turbulent ones, using the SST k-ω model was of great importance in conjunction with studying local heat transfer. The analysis was performed in the flow region where the Raynaud number is limited to values 1800-3700. The results of the analysis revealed that the quantity and extent of vortex pairs increase with increasing rib height (H_{rib}) and that the velocity of the fluid near the bottom surface of the channel and the amount of turbulence caused by the eddy pairs are the most important in influencing the magnitude of heat exchange [12]. Studies and tests were conducted on the

modified PV unit, which confirmed that its efficiency reached better rates as a result of the dual use of the two forms of electrical and thermal energy together resulting from the modified panel. In addition to improving cell performance at low cost, the use of water cooling system provides reverse osmosis technology to cool the water through preheating, which is more economical [13-16].

Many reviews have shown that active cooling, because it consumes a fraction of the energy produced or requires external power, is more expensive and more complex than passive cooling, depending on the type and installation of the system, so it is an uneconomical system. Air cooling is also less efficient than water cooling. In addition, the results appeared that reducing the average surface temperature (T_{ave}) of the photovoltaic panel depends greatly on the coolant flow rate (Q), which by increasing it to the optimal rates increases the cell production and thus improves the efficiency [17, 18]. Cleaning solar panels with water and materials used for washing household dishes was used to increase their productivity, which also cools them, and the results were a clear increase in production power [19].

Regarding the use of thermoelectric generators, an experimental application has been used to collect dispersed heat using radiation heat exchange [20]. Recent research such as that using a heat sink with vertical fins attached to the hot side of a thermoelectric generating unit versus a radiant heat source has been used to increase the amount of heat reaching the hot side through radiation. The results showed the superiority of this type over units that use horizontal fins for the same gap between the radiation source and the hot side [21].

Most previous studies and research, despite their significant number, aimed to create the best operating conditions close to the ideal conditions for operating photovoltaic panels, or those that examined the possibility of increasing their efficiency, but there are still possibilities for research and development in them. This research aims to contribute to increasing the efficiency of PV panel and utilizing the heat extracted from the water cooling system in creating a hybrid electrical generation system consisting of photovoltaic panel and thermoelectric units. This model includes a heat exchanger designed to be part of the PV panel without the use of a heat-absorbing portion that separates the back wall of the panel from the water.

2. SIMULATION STUDY

2.1 Description of numerical model

Figure 1 shows a model of a new PV/T hybrid system that requires an analytical test for it and for the rest of the cooler box models, part of which is shown in Figure 2, the dimensions of which change according to the depth of the channel, the number of ribs and their length, as shown in Table 1, so that the best performing one can be selected and manufactured for practical comparison. This model consists of the layers of the photovoltaic panel shown in Table 2, in addition to the cooling box referred to above. This section deals with the numerical simulation of the coolant flow through the cooling box for each model after drawing it in the Solidworks program explorer 2015, entering it into the ANSYS software (version R19.2), and performing the analysis using CFD technology. The effect of the ribbed fins of the heat exchanger on the heat transfer rate and the percentage of improvement in the heat transfer coefficient were studied compared to a heat exchanger without ribs, that is, with crossed fins only. The effect of changing both the water flow rate and the intensity of the radiation falling on the panel was also studied. The flow rates selected were 0.3, 0.5, 1, 2, 3 and 4 L/min, and the radiation intensity was 400, 600, 813 and 1035 W/m², in addition to the ambient air temperature and incoming water temperature under specified working conditions.

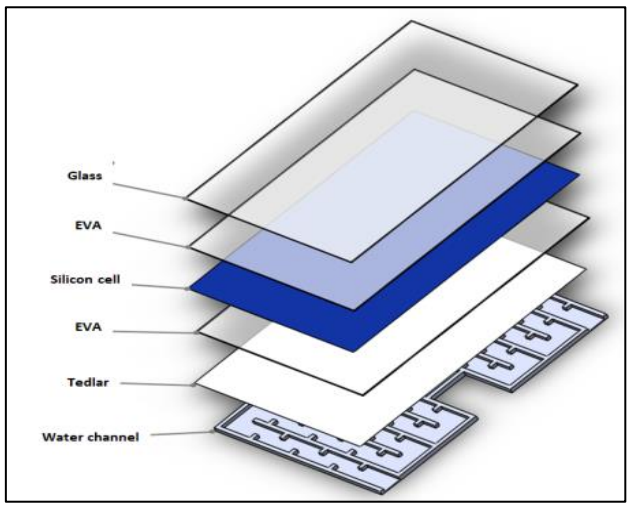

Figure 1. Layer assembly diagram of the hybrid PV/T system

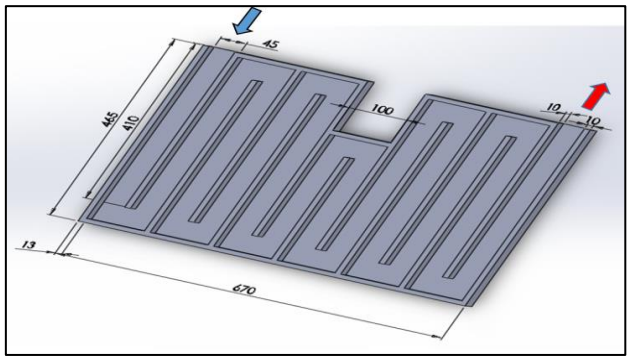

(a) Model-1

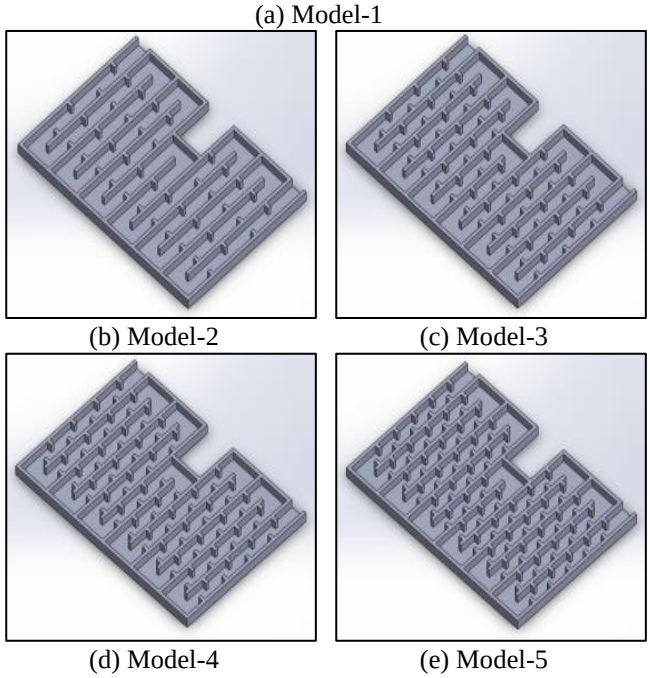

(b) Model-2 (c) Model-3

(d) Model-4 (e) Model-5

Figure 2. Schematic diagram of cooler box models

Table 1. Components and characteristics of cooler box

Case	Box Dimensions (mm)	Rib Dimensions (mm)	Channel Dimension (mm)	D_h (mm)
1	670 × 465 × 8	15 × 10 × 5 25 × 10 × 5 30 × 10 × 5	45 × 5	9.0
2	670 × 465 × 13	15 × 10 × 10 25 × 10 × 10 30 × 10 × 10	45 × 10	16.36
3	670 × 465 × 18	15 × 10 × 15 25 × 10 × 15 30 × 10 × 15	45 × 15	22.50

Table 2. Characteristics of the photovoltaic panel [22, 23]

Layer	Thickness (mm)	k (W/m. K)	C_p (J/kg K)	ρ (kg/m³)
glass	3.00	1.00	500	3000
EVA	0.025	0.311	2090	950
PV cells	0.300	148	700	2330
tedlar	0.050	0.15	1250	1200

This type of simulation requires entering data and properties of the layers of the photovoltaic panel and the cooling box, in addition to the surrounding environment data, such as radiation and temperature of the incoming water, air, and the convective heat transfer coefficient (h_a), which is calculated from knowledge of the wind speed in the work environment according to the experimental equation below:

$$h_a = 5.7 + 3.8(V_{wind}) \quad (1)$$

where, V_{wind} is the wind velocity around the PV/T collector (m/s) [24]. It also requires determining the type of flow by knowing the Reynolds number, as the flow is in its stratified state if the Reynolds number ≤ 2000, and if it exceeds this number, it turns into turbulent flow [25].

Readings were obtained from the experimental test inputs for later comparison, based on the scientific and practical constants of both tests. The constant properties of water, such as coefficient of thermal conductivity (k), specific heat (C_p), dynamic viscosity (μ), and density (ρ), were chosen to have the following values: 0.6 (W/mK), 4182 (J/kg-K), 0.001003 (kg/m-s), and 998.2 (kg/m³), respectively.

2.2 Grid independency

The quadrilateral mesh model in the ANSYS software consists of several nodes and elements for the liquid and solid parts, in addition to the connection elements. For the regular model without ribs, the number reaches 40,840 nodes and 27,540 elements for the liquid, while it reaches 174,900 nodes and 86,110 elements for the solid parts, while the number of connection elements is 1,156,544. Figure 3 shows the sizes of the mesh chosen according to the data in Table 3 under a radiation intensity of 1000 W/m². It shows how to choose the optimal mesh for the model based on the quality of the elements, which ranges between (0-1) [25] and the preferred optimal value is the closer it is to 1.

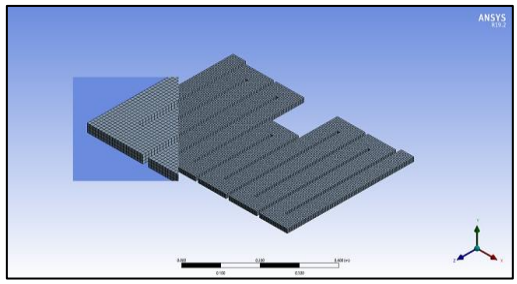

(a) water

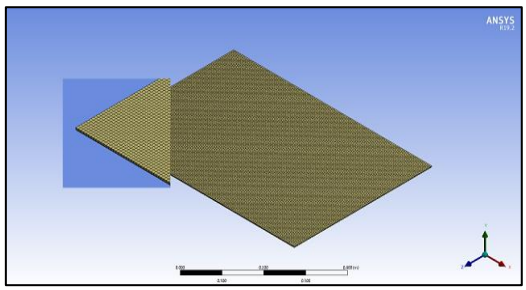

(b) PV panel

Figure 3. Mish generation

2.3 Governing equations

In this segment, the Navier Stokes equations are solved using the CFD model for 3D equations, which is most frequently used in software to forecast the temperature distribution over the whole PV panel and through the coolant;

Equation of continuity:

$$(\nabla \cdot \vec{V}) = \left[\frac{\partial}{\partial x}(\rho u) + \frac{\partial}{\partial y}(\rho v) + \frac{\partial}{\partial z}(\rho w)\right]\vec{V} \quad (2)$$

Equation of momentum:

$$(\vec{V}.\nabla)\vec{V} = -\left(\nabla p - \mu\nabla^2\vec{V}\right) \quad (3)$$

Table 3. Choosing the optimum mesh

Element Size (mm)		4.25	4.5	5.1	5.5	6.0	6.5	Optimum 4.25 + 5.1
Solar radiation (W/m²)		1000	1000	1000	1000	1000	1000	1000
PV panel	Nodes	174900	156000	121624	105780	89428	75920	174900
	Elements	86110	76735	59696	51850	43758	37080	86110
Element quality (PV)	Min.	**0.01798**	0.0102	0.00898	0.00838	0.00769	0.007085	0.01798
	Max.	**0.92856**	0.9058	0.08495	0.81556	0.77221	0.72992	0.92856
Water	Nodes	72965	50908	40840	34236	30248	18498	40840
	Elements	53416	34680	27540	22800	20037	10704	27540
Element quality (Water)	Min.	0.96174	0.9923	**0.99925**	0.99056	0.76209	0.91224	0.99925
	Max.	0.99248	0.9944	**1.0**	0.99346	0.99123	0.98862	1.0
Contact elements		1156544	103076	802294	696860	588384	498622	1156544
PV average temp.°C		37.572	36.540	36.389	36.468	36.444	37.55	36.368
Outlet water temp.°C		47.13	43.61	43.15	43.38	43.13	43.15	43.45

Conservation of energy for solid:

$$\nabla.(k.\nabla T) = 0 \tag{4}$$

where, $\vec{V}$ is the velocity vector (m/s) in x, y and z directions that denoted by u, v and w respectively, μ is the dynamic viscosity (kg/m. sec), k is the thermal conductivity (W/m. K), T is the temperature (K), ρ is the density (kg/m^3) and p is pressure measured in Pascal. To apply the above equations, some assumptions necessary to complete the solution must be taken into account, which are:

- Three dimensions incompressible steady state.
- Three dimensions thermal conductivity via PV panels.
- To locate every property, use the average temperature.

The electrical efficiency of the PV panel can be determined by using the average temperature of this panel as a function of the following equation [26].

$$\eta_{\text{electrical}} = \eta_{\text{ref}} \left(1 - 0.0045\left(T_{pv(\text{ ave })} - 298\right)\right) \tag{5}$$

where, η_{ref} is the PV module's efficiency at the reference temperature and $T_{pv(ave)}$ represents the average PV temperature (K) [27, 28].

3. EXPERIMENTAL RESEARCH

This section includes preparing and implementing the experimental model to achieve the study objective. The practical part is divided into two stages. The first represents a study of the possibility of increasing the production efficiency of PV panel by reducing their temperature and improving heat transfer to a cross-flow heat exchanger using rectangular ribbed fins installed on its back wall, as indicated in the numerical part. It is also possible to determine the degree of agreement between the results of both tests under the same working conditions. While the second stage includes adding thermoelectric generator units in the hottest part near the outlet of the heat exchanger and its back wall to demonstrate the possibility of generating additional energy.

3.1 Experimental rig

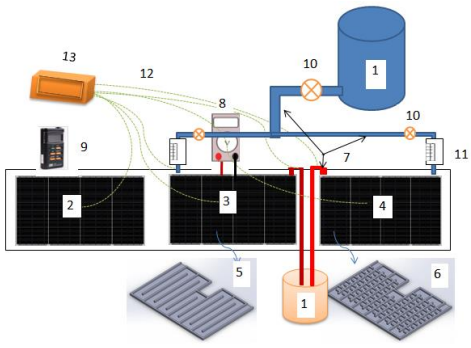

1	Water tanks.	8	Voltmeter.
2	PV panel without cooling.	9	Solar power meter.
3	PV panel with cooling (without ribs).	10	Regulator valves.
4	PV panel with cooling (with ribs).	11	Water flow meter.
5	Cooling box (radiator) without ribs.	12	Wires of thermocouple.
6	Cooling box (radiator) with ribs.	13	Temperature recorder.
7	Tubes.		

Figure 4. The schematic diagram of experimental rig

Figure 4 displays a diagram of the experimental rig, and Figure 5 shows the image of this device, which consists of the main test section (PV panels), tubes with different diameters, regulator valves, water tanks and measuring units.

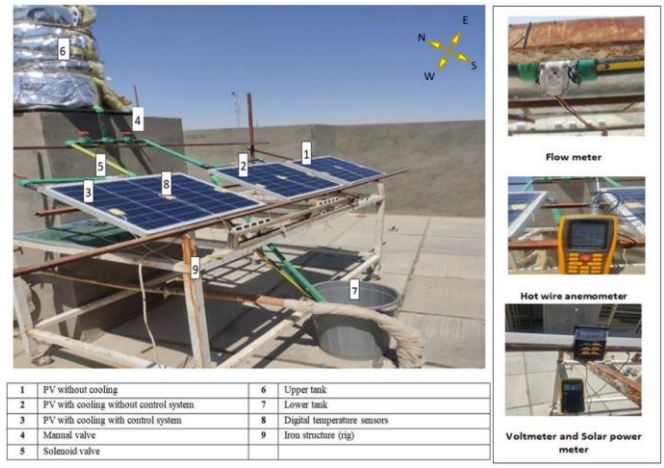

1	PV without cooling	6	Upper tank
2	PV with cooling without control system	7	Lower tank
3	PV with cooling with control system	8	Digital temperature sensors
4	Manual valve	9	Iron structure (rig)
5	Solenoid valve		

Figure 5. Photo of experimental device

3.1.1 Main test section (PV panels)

The main section of the experimental test represents the basis of the design, or what is called the core of the work under investigation, in order to identify its outputs and their compatibility with the applicable standards, as well as compare them with other analytical standards.

Figure 6. Photo of panel and its characteristics

Figure 7. Images of aluminum cooling box

This section includes three PV panels that are identical in terms of production, dimensions and components. Figure 6 shows one panel and its features. All of this work is done to

create a realistic, practical scientific comparison that shows how each can be improved in order to achieve the testing objectives through experimentation.

The first panel represents a conventional PV panel does not have any cooling mechanism. In contrast, the second and third panels have an aluminum cooling box as shown in Figure 7 attached to their back walls. The second panel has crossed fins, creating rectangular channels measuring 45*10 mm from the inlet to the outlet, as shown in Figure 8(a). The third panel is similar to the second panel, but it also has ribs for the fins. The dimensions of the rib are 30*10*10 mm (length*width*height) and the distance between each two ribs is 60 mm, as shown in Figure 8(b).

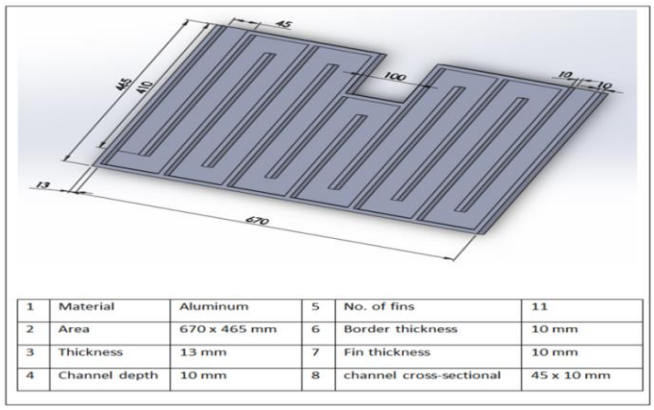

1	Material	Aluminum	5	No. of fins	11
2	Area	670 x 465 mm	6	Border thickness	10 mm
3	Thickness	13 mm	7	Fin thickness	10 mm
4	Channel depth	10 mm	8	channel cross-sectional	45 x 10 mm

(a)

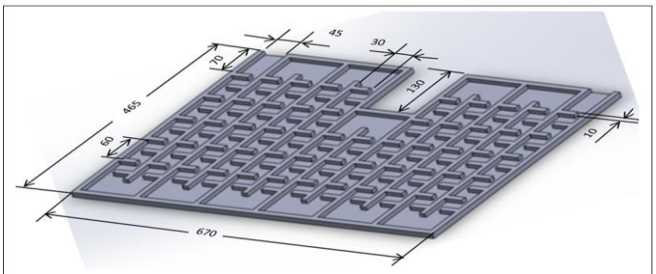

1	Material	Aluminum	6	No. of fins	11
2	Area	670 x 465 mm	7	Border thickness	10 mm
3	Thickness	13 mm	8	Distance between 2 ribs	60 mm
4	Channel depth	10 mm	9	channel cross-sectional	45 x 10 mm
5	No. of ribs	112	10	Rib dimensions	30x10x10 mm

(b)

Figure 8. Diagrammatic drawing of an aluminum cooler box without ribs (NRFCB) and with ribs (RFCB)

3.1.2 Units of measurement

In the experimental tests, different measuring devices were used that were compatible with the nature and pattern of the test and the results being investigated. In this study, different devices were used, including temperature measuring devices, solar radiation intensity measuring devices, cold water flow rate measuring devices, in addition to a device for measuring the voltage and current coming out of the photovoltaic panels. Figure 9 shows all the devices, the calibration of which was taken into consideration to ensure accuracy and reliability.

Unit of temperature measurement. To know the temperature distribution ($T_1, T_2, T_3, \ldots \ldots T_n$) for each of the three panel surfaces used in the experimental test, the ambient air temperature, the temperature of the cold water entering the cooler box and the hot water exiting it in each of the two panels equipped with cooling systems, 14 digital temperature sensors of type TPM-10 with an accuracy of ± 1°C were used.

Solar power meter. A solar power meter (type TES 1333) was utilized to measure the amount of solar radiation falling on the test panels in the work environment.

Water flow meter. A YF-S401 sensor was used, which is simple and very similar to the larger type of the same family, the YF-S201, except that some improvements have been made to it to make it more suitable for measuring low flows of 0.3-6 L /min with a higher signal pulse per liter measured. It should also be noted that it can operate under pressure up to 0.8 MPa.

Wind speed measuring device. One of the most important factors affecting the amount of convection coefficient at any solar cell test site is the wind speed at that location, so it requires the use of an accurate instrument to measure wind speed. Among these devices, a hot wire anemometer (type GM8903) was used.

Voltmeter. Because the current test requires knowing the efficiency of the solar panels in practice, which means knowing both the voltage and current, in addition to knowing the temperature of random points along the surface of the solar panel, in addition to the digital sensors installed at the specified points to ensure that the test path is proceeding correctly and harmoniously. So, a multimeter voltmeter of the type (DT9208SA).

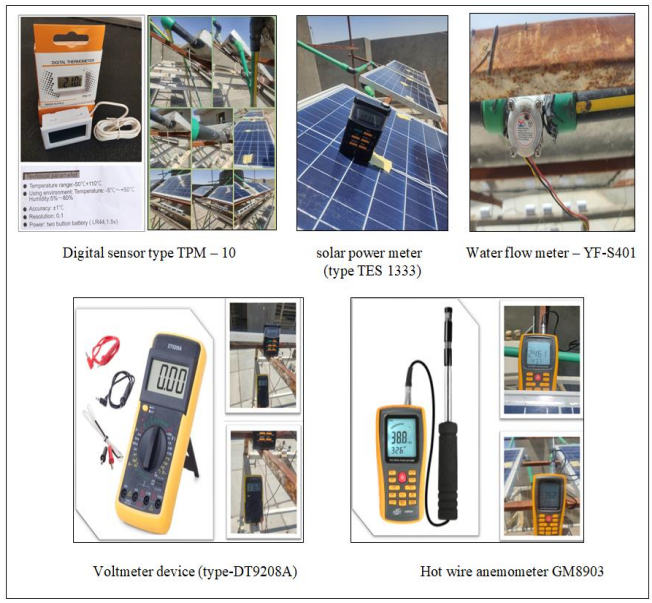

Figure 9. Units of measurement

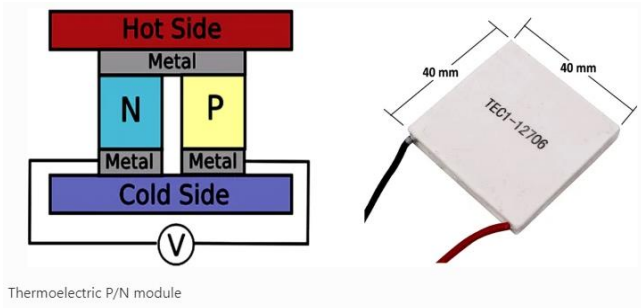

Figure 10. Thermoelectric generator

3.2 Add thermoelectric generator (TEG)

In this part of the practical test, 8 units of thermoelectric generators shown in Figure 10 and their characteristics shown

in Table 4 are added, which are placed on the back wall of the ribbed fin cooler box.

The TEG units are placed in a strip manner on the hottest part of the wall, which is located at the end of the cooling box near the hot water outlet hole, as shown in Figure 11.

Table 4. TEG characteristics under standard conditions [29]

Parameter	Value	
TEG module dimensions	(40 × 40) (mm)	
Leg cross sectional area (CS)	(0.001 × 0.001) (m)	
Leg's length	0.0015 (m)	
Seebeck coefficient	p-type	223.2 μVK^{-1}
	n-type	-187.7 μVK^{-1}
Electrical resistivity	p-type	0.183 μV.m
	n-type	0.153 μV.m
Thermal conductivity	p-type	1.68 (W/m K)
	n-type	1.64 (W/m K)

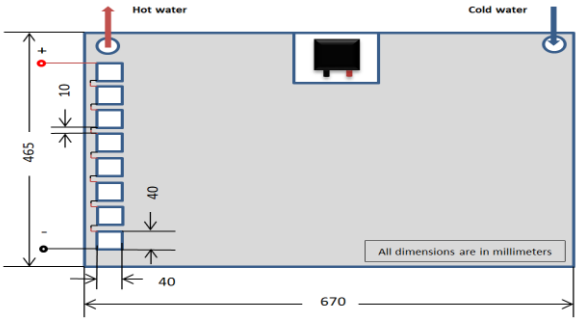

Figure 11. Place and method of connecting TEGs

The TEG units are fixed to the back wall with a thermal adhesive after adding thermal cream between the ceramic piece that represents the hot side of the TEG and the aluminum that represents the heat dissipating part of the back wall to ensure greater thermal conductivity and reduce the roughness of the two surfaces. TEG modules are connected in series to obtain greater voltages at the same current per module.

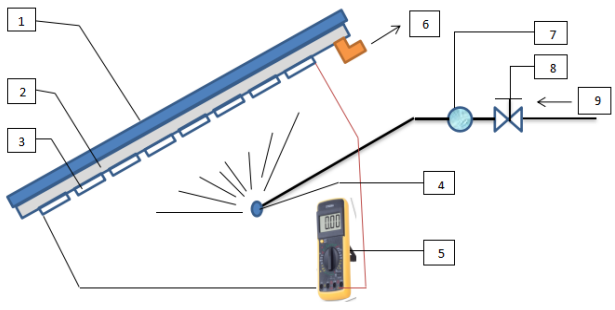

1	photovoltaic panel	6	Hot water outlet
2	Cooler box (radiator)	7	Water flow meter
3	Thermoelectric generator (TEG)	8	Flow regulating valve
4	Nozzle	9	Water from the tank
5	Multimeter voltmeter		

Figure 12. Schematic layout of the second part of the experimental setup

The output test of TEG modules is carried out in two ways. The first is to leave the other surface of the TEG modules exposed to the temperature and wind speed of the surrounding air without any additives. The second method includes adding a water spray system with the same temperature as the cooling water that enters the cooling box after connecting a new water pipe from the upper tank to take advantage of the water pressure in it to feed the sprinkler as shown in Figures 12 and 13.

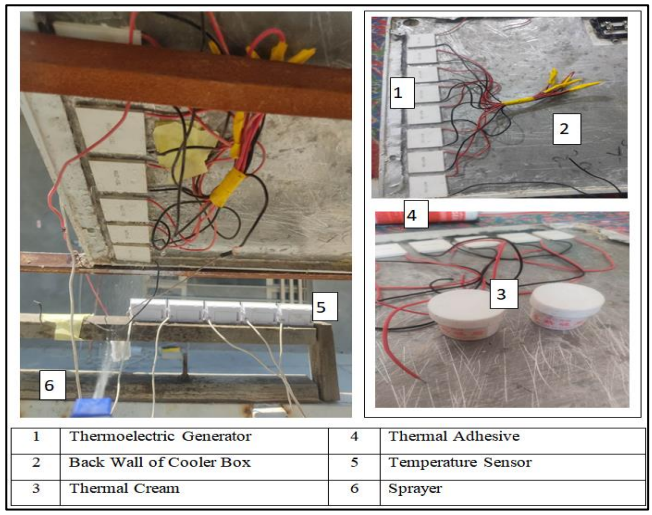

1	Thermoelectric Generator	4	Thermal Adhesive
2	Back Wall of Cooler Box	5	Temperature Sensor
3	Thermal Cream	6	Sprayer

Figure 13. Photo of the second part of the experimental setup

3.3 System's performance calculation

Tests contribute to obtaining a lot of data that is of great importance in determining the efficiency and performance of the models that are subject to testing. Regarding experimental tests of PV panels, the important outcome investigated is the amount of electrical energy produced and how efficiently the panel sustains this production, which is mainly affected by the average temperature of the PV panel. The efficiency is calculated practically using the general electrical energy calculation law, and then the electrical efficiency is calculated using the following equations:

The output power of the PV panel.

$$P_{output} = I_{measured} * V_{measured} \quad (6)$$

The electrical efficiency of the PV panel.

$$\eta_{electrical\_PV} = P_{output} / P_{from\ radiation} = \left(I_{measured} * V_{measured}\right) / G.A_{panel} \quad (7)$$

where, P_{output} represents the output power of the PV panel at the output current ($I_{measured}$) and output voltage ($V_{measured}$) of the panel. The solar irradiation over the entire surface area of the panel (A_{panel}) is denoted by G.

To practically calculate the power produced by thermoelectric generation units (TEGs), the general electrical power calculation law is also used.

The output power of the TEGs.

$$P_{TEG} = I_{TEG} * V_{TEG} \quad (8)$$

The total output power of the PV panel + TEGs.

$$P_{(PVpanel+TEGs)} = P_{output} + P_{TEG} \quad (9)$$

The total electrical efficiency of the PV panel + TEGs.

$$\eta_{\text{electrical }(PV+TEGs)} = P_{(\text{PVpanel+TEGs})} / G \cdot A_{\text{panel}} \quad (10)$$

4. RESULTS AND DISCUSSION

4.1 Effect of water flow variation (Q)

Figures 14 to 17 show the difference in average PV panel temperature and outlet water temperature for both numerical and experimental testing and for two cooler box models, NRFCB and RFCB, and also show how similar and different they are. This comparison was performed under constant solar heat fluxes (400, 600, 813 and 1035 W/m²) and for different flow rate values (0.3, 0.5, 1, 2, 3 and 4 L/min). Both NRFCB and RFCB models behave similarly in terms of temperature changes for both tests, except for some differences in temperature values which are lower in the numerical test than those obtained in the experimental part. Also, average PV panel temperature for both models was lower compared to traditional non-cooled panel.

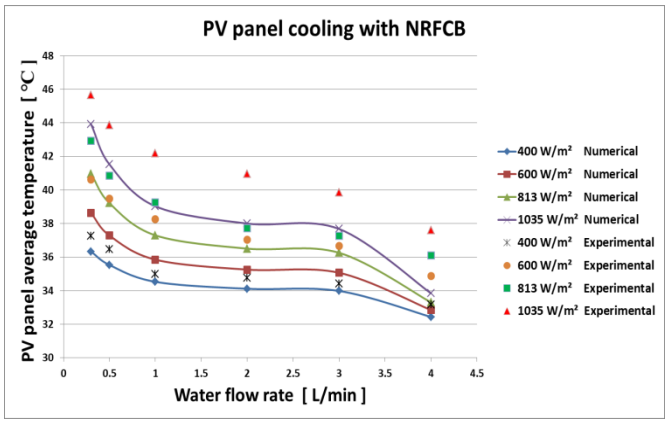

Figure 14. Comparison of numerical and experimental results for the PV panel temperature of the NRFCB model

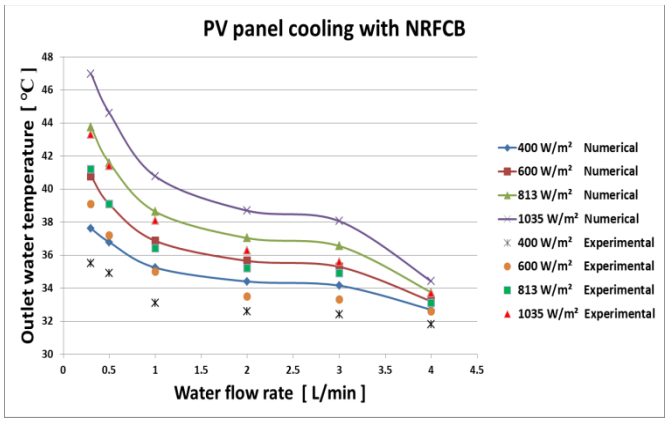

Figure 15. Comparison of numerical and experimental results for the outlet water temperature of the NRFCB model

The conventional panel recorded the highest value of the average panel temperature for both experimental and numerical testing under the radiation rate of 1035 W/m², which reached 65.532°C and 67.5°C, and its lowest value under the radiation intensity of 400 W/m², which was 45.247°C and 44.4°C respectively.

For the two models, NRFCB and RFCB, the highest value of average PV panel temperature was recorded under the radiation level of 1035 W/m² and at Q=0.3 L/min, where it reached 45.667°C and 43.867°C in the experimental test, while it decreased to 43.926°C and 41.612°C in numerical testing. Also, the lowest value was recorded under the radiation level of 400 W/m² and at Q=4 L/min, where it was 37.6°C and 35.9°C for the experimental test and 32.439°C and 32.082°C for the numerical test. As for the temperature of the outlet water, its highest value was recorded under the radiation rate of 1035 W/m² at Q=0.3 L/min, where it reached 43.3°C and 41.7°C experimentally, 46.98°C and 45.06°C numerically. While its lowest value was recorded under a radiation rate of 400 W/m² at Q=4 L/min, and it was 31.8°C and 31.6°C experimentally, 32.69°C, and 32.22°C numerically in both models, respectively.

It is clear from the above that as the incoming radiation remains constant and the flow rate increases, the temperature of the PV panel and the outlet water decreases significantly until it converges to water inlet temperature which was 31.5°C.

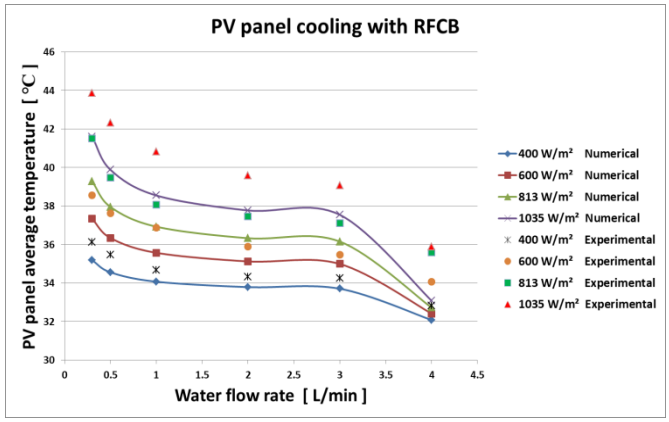

Figure 16. Comparison of numerical and experimental results for the PV panel temperature of the RFCB model

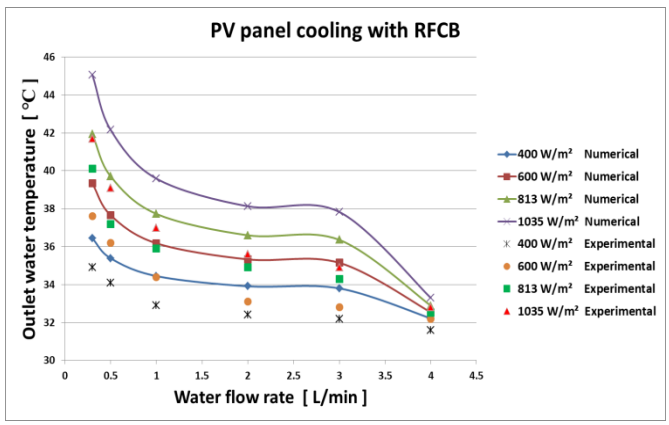

Figure 17. Comparison of numerical and experimental results for the outlet water temperature of the RFCB model

Despite the clear convergence between the results of experimental and numerical tests, there is a slight deviation in the results. The reason for this deviation is due to several influences that accompanied the experimental test and not the numerical test, in which the surrounding environment has the greatest influence. The wind speed was adopted as a numerically constant speed while it was practically variable during the test period, so it was adopted as an average, and this clearly affects the convective heat transfer (h) to the space surrounding the photovoltaic panel, which in turn affects the

temperature values. Also, the calculation of losses from the edges to the experimental workplace was neglected, and this is most evident in the ports of the panel cooling boxes, noting that the average panel temperature was calculated as an average of three points for each panel in practice, while the entire surface area of the painting is digitally measured. Figure 18 shows the effect of increasing solar radiation intensity on increasing the standard deviation of the panel surface temperatures and water exiting the cooling boxes for both the NRFCB and RFCB models. On the other hand, Table 5 shows the deviation values of the average PV panel surface temperatures for the RFCB model, while the standard deviation for the other model and the outlet water for both models were calculated in the same way.

Table 5. Error ratio between numerical and experimental results for PV panel temperature for the RFCB model

Flow Rate L/min	$T_{PV\ (average)}$ ℃ Num.	Exp.	Absolute Error (X)%	X^2	Standard Error (σ)%
			For 400 W/m²		
0.3	35.19	36.133	2.60	6.76	
0.5	34.56	35.467	2.55	6.50	$\sigma = \sqrt{\frac{\Sigma x^2 - n\bar{x}}{n-1}}$
1	34.074	34.667	1.14	1.30	
2	33.79	34.333	1.58	2.49	
3	33.708	34.267	1.63	2.65	
4	32.082	32.833	2.28	5.19	
			$\bar{x} = \Sigma x /n =$ 1.96%	ΣX^2 =24.89	1.62%
			For 600 W/m²		
0.3	37.342	38.567	3.17	10.04	
0.5	36.344	37.633	3.42	11.69	$\sigma = \sqrt{\frac{\Sigma x^2 - n\bar{x}}{n-1}}$
1	35.574	36.867	3.50	12.25	
2	35.124	35.90	2.16	4.66	
3	34.994	35.467	1.33	1.76	
4	32.418	34.067	4.84	23.42	
			$\bar{x} = \Sigma x /n =$ 3.07%	ΣX^2 =63.82	3.01%
			For 813 W/m²		
0.3	39.287	41.50	5.33	28.40	
0.5	37.957	39.467	1.32	1.74	$\sigma = \sqrt{\frac{\Sigma x^2 - n\bar{x}}{n-1}}$
1	36.93	38.067	2.98	8.88	
2	36.331	37.467	3.03	9.18	
3	36.157	37.10	2.54	6.45	
4	32.725	35.60	8.07	65.12	
			$\bar{x} = \Sigma x /n =$ 3.87%	ΣX^2 =129.77	4.61%
			For 1035 W/m²		
Flow rate L/min	$T_{PV\ (average)}$ ℃ **Num.**	**Exp.**	**Absolute error (X)%**	X^2	**Standard error (σ)%**
0.3	41.612	43.867	5.14	26.42	
0.5	39.884	42.333	5.78	33.40	$\sigma = \sqrt{\frac{\Sigma x^2 - n\bar{x}}{n-1}}$
1	38.551	40.833	5.58	31.13	
2	37.773	39.60	4.61	21.25	
3	37.546	39.067	3.89	15.13	
4	33.088	35.90	7.83	61.30	
			$\bar{x} = \Sigma x /n =$ 5.47%	ΣX^2 =188.63	5.58%

4.2 Effect of heat flux variation

Figure 19 clearly shows the degree of convergence of the experimental results with the computational (numerical) results made for three panels under similar working conditions, namely, the conventional panel (ref.) and the two water-cooled panels according to the NRFCB and RFCB models. A comparison was made of the results of the relationship between the average panel temperature change and the heat flux at constant values of flow (0.3, 0.5, 1, 2, 3 and 4 L /min). The results showed that the largest difference for the two tests is under the heat flux of 1035 W/m², as the difference in the traditional panel was about 1.86°C, after it was the lowest possible degree under the radiation intensity of W/m², when it was 0.84°C.

As for the NRFCB and RFCB models, the largest difference was also under the radiation intensity 1035 W/m², where the difference was 1.74, 2.33, 3.16, 2.96, 2.18, and 3.75°C for the NRFCB model and 2.25, 2.44, 2.28, 1.82, 1.52, and 2.81°C for the RFCB model for values of water flow 0.3, 0.5, 1, 2, 3 and 4 L /min, respectively. The reasons for these differences are as stated in paragraph (4.1), noting that these deviations are within and below the internationally permitted rates.

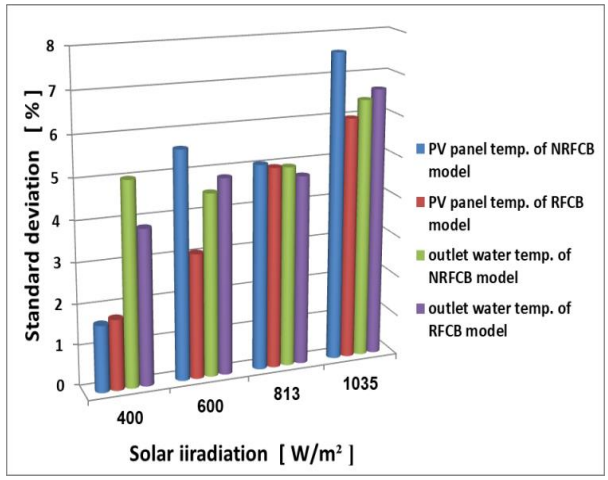

Figure 18. Effect of radiation intensity on the percentage of standard error

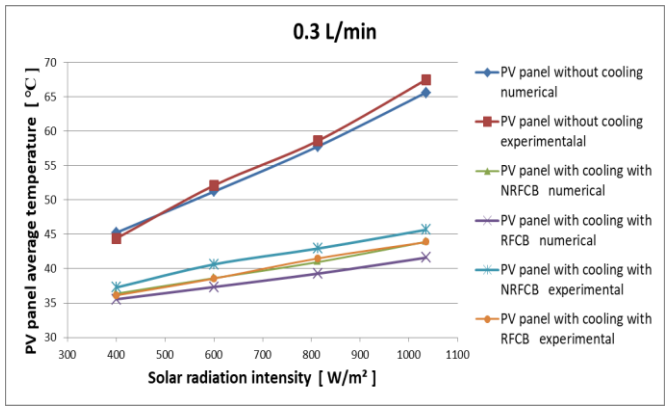

(a)

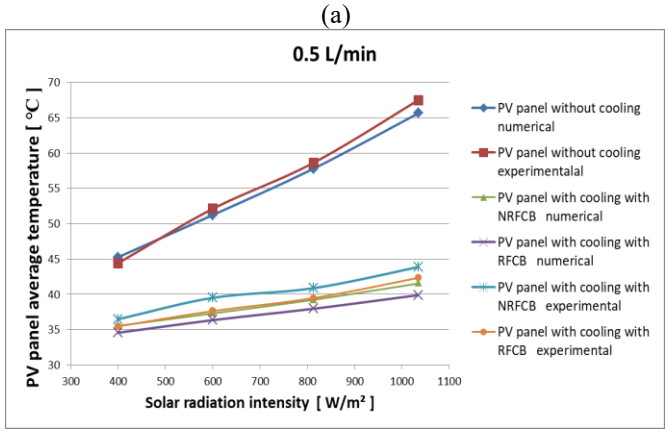

(b)

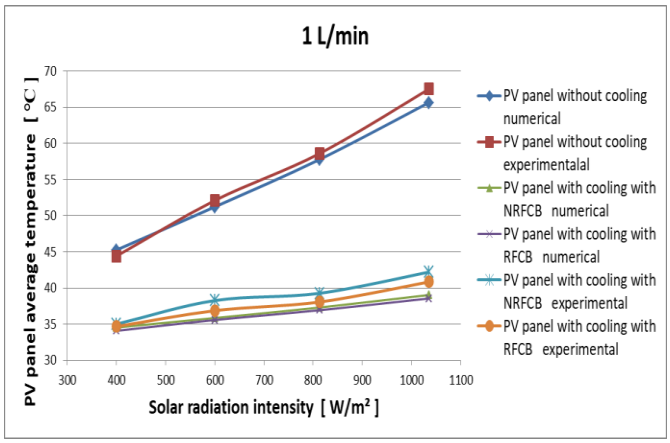

(c)

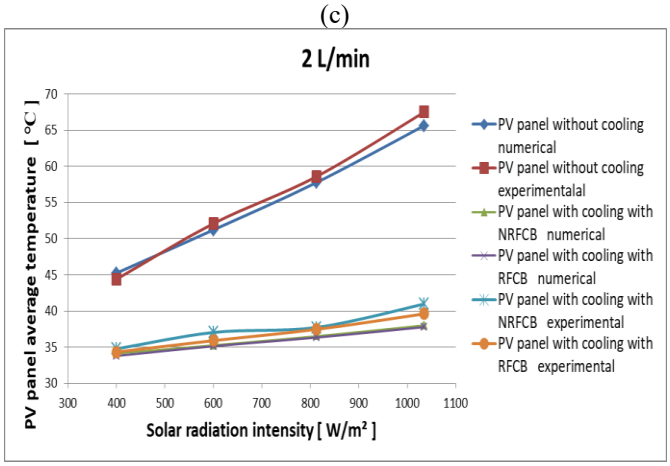

(d)

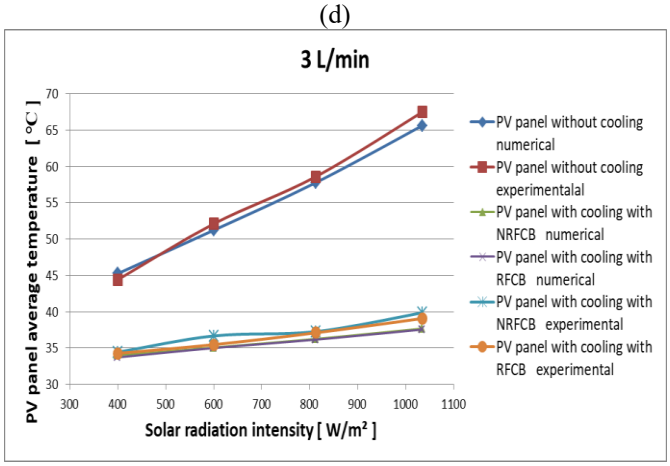

(e)

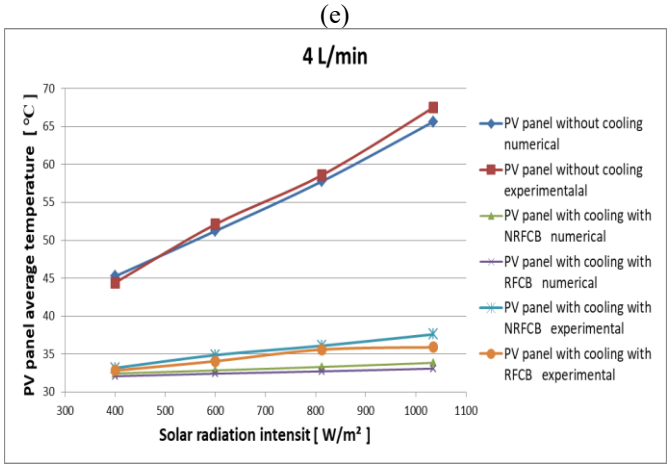

(f)

Figure 19. Change in average temperature of PV panels with change in solar radiation for conventional panel (no cooling), with NRFCB and with RFCB at different flow rate

4.3 Effect add the TEG modules

Figure 20 shows the change in the amount of power produced from 8 thermoelectric generating units (TEG) placed at the end of a cooling box of the RFCB model to take advantage of the heat accumulated at the end of the box before leaving it, noting that the test was carried out under a low flow rate of 0.5 L /min to ensure obtaining a temperature difference that can be used in generation.

Two methods of cooling the TEGs were tested, the first is by leaving them exposed to the surrounding air, and the second method is by using water spraying on the cold side of the TEGs to create a greater difference in the necessary temperatures for generation, as well as benefiting from spraying water to cool the last part of the box, even if it is simple. The curves show the test results for the day on July 15 th, 2023 in the city of Kut in Iraq. These curves showed that the air cooling achieved only a very small part of the power due to the inability to obtain a significant temperature difference necessary for the operation of the TEGs. As for the use of water spray, a good power was obtained, as it was highest at 11:40 and 14:30, reaching 0.142 and 0.144 W, respectively.

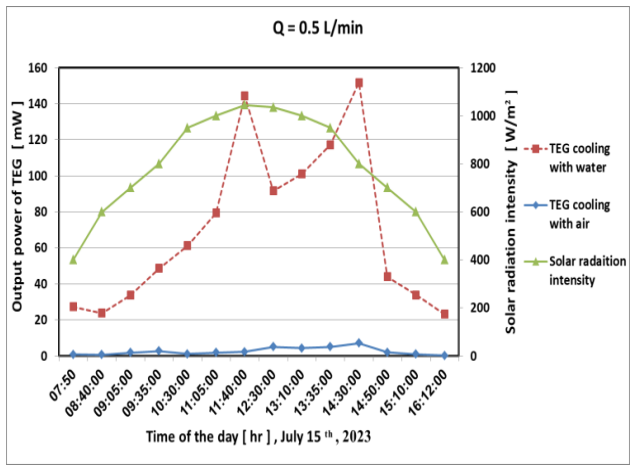

Figure 20. The power generated from the TEG modules, according to the type of cooling used, during the day on July 15 th, 2023

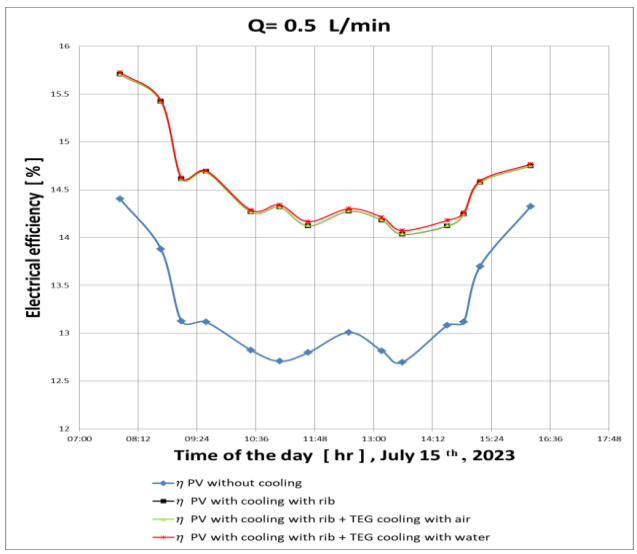

Figure 21. Variation of electrical efficiency during daylight hours on July 15 th, 2023 for both the conventional PV panel and RFCB (three cases) for Q = 0.5 L /min

4.4 Electrical efficiency change during daylight hours on 15 July 2023

Figure 21 shows the amount of change in the electrical efficiency value during the daylight hours on July 15, 2023 for each of the traditional reference panel (without cooling) and the cooled panel according to the RFCB model, in addition to the RFCB model, in addition to the thermoelectric generation units, which are cooled once with air and another one by spraying water.

The results showed that the panel cooled according to the RFCB + TEGs model and using the spraying method is the highest efficiency, as adding the power generated from the TEGs units is an improvement, despite its simplicity, it is a clear addition and is suitable for hot summer weather with high temperatures, as shown in Figure 20, which shows the amount of temperature and radiation intensity for the test day, as well as the small number of units and the size of the panel used in the study. The rate of improvement in efficiency ranged between 0.1%-0.41%.

5. VALIDATION

From Figure 21 and in comparison, with many studies, including Shalaby et al. [13] and Syafiqah et al. [30], which achieved an improvement in electrical efficiency of about 14.1% and 14% respectively by cooling the back wall of the photovoltaic panel with water, while the current study achieved 14.65%, which indicates the correct direction of the study, taking into account the conditions of the test entrance.

6. CONCLUSION

Conclusions were reached by analyzing both the results of the first part (preliminary numerical analysis), on the basis of which Model 5 was chosen, which performed best, and the results of experimental and numerical tests for the chosen model, as well as the hybrid generation of electrical energy generated by adding a number of TEG units. To the back wall of the PV panel cooler box are:

Good agreement was reached when comparing the numerical and experimental results, as the standard error does not exceed 7.58% in the worst case, which is for the average temperature of the solar panel at the highest solar radiation level of 1035 W/m². This is due to the direct and indirect effect of the conditions of the real working environment represented by the instability of the wind speed and the temperature of the external environment, thus changing the value of the heat transfer coefficient in practice. Therefore, more tests must be conducted inside the laboratory to maintain the working environment.

Both traditional panel and panels cooled according to the NRFCB model and the RFCB model achieved their highest electrical efficiency under a solar radiation rate of 400 W/m², reaching 14.44%, 15.37%, and 15.49%, respectively. While the lowest efficiency achieved was at a solar radiation rate of 1035 W/m², reaching 12.97%. 14.87% and 15.06%, respectively. The results also indicate that the panel cooled according to the RFCB model achieved the best improvement rate compared to the performance of the traditional panel and the panel cooled according to the NRFCB model, which amounted to 13.87% and 1.26%, respectively, under solar radiation of 1035 W/m² and a flow rate of 4 L/min. It is noted that the effect of using only water has achieved a significant improvement for the RFCB model, which requires studying the effect of nanofluids with different concentrations in future research.

The addition of 8 of TEGs using water spray to cool the cold side achieved a significant power compared to high temperatures and wind fluctuations, as the highest power was at 11:40 and 14:30, which amounted to 0.142 and 0.144 W, respectively.

The rate of improvement in the electrical efficiency ($\eta_{electrical}$) of the cooled panel according to the RFCB model with the addition of TEGs ranged between 0.1%-0.41% during the day of July 15, 2023, at Q=0.5 L /min. Although the improvement is slight for the performance of a limited number of TEGs in a hot and volatile summer, it indicates better effectiveness, especially if we take into account the addition of heat sinks to the cool side of the TEGs in addition to the water mist.

The desire for increased use of solar panels and the rapid growth in this sector necessitate finding an integrated model in terms of little sensitivity to heat associated with radiation, especially in the field of operating artesian wells in areas far from energy sources and where cooling water is available.

REFERENCES

[1] Mohamed, R.G., Mohsen, A., Hegazy, R. (2022). Temperature distribution modeling of PV and cooling water PV/T collectors through thin and thick cooling cross-fined channel box. Energy Reports, 8: 1144-1153. https://doi.org/10.1016/j.egyr.2021.11.061

[2] Kemal, B., İsmail, E. (2023). Effects of cooling on performance of photovoltaic/thermal (PV/T) solar panels: A comprehensive review. Solar Energy, 262: 111829. https://doi.org/10.1016/j.solener.2023.111829

[3] Hashim, A.H., Ali, H.N., Ruaa, A.A. (2017). Improving the hybrid photovoltaic/thermal system performance using water-cooling technique and Zn-H_2O nanofluid. Hindawi International Journal of Photoenergy, 2017(1): 2-14. https://doi.org/10.1155/2017/6919054

[4] Elmouazen, H., Zhang, X.B., Gibreel, M. (2022). Heat transfer enhancement of regenerative-cooled system with various V-rib cross-sections. Applied Thermal Engineering. http://doi.org/10.2139/ssrn.4171530

[5] Elmouazen, H., Zhang, X.B., Gibreel, M., Ali, M. (2022). Numerical investigation of pentagonal V-shape ribs to enhance heat transfer in hydrogen rocket engine cooling channels. International Journal of Hydrogen Energy, 47(56): 23871-23886. https://doi.org/10.1016/j.ijhydene.2022.05.146

[6] Natthaporn, K., Tanakorn, S., Pathomporn, N., Chayut, N. (2020). Flow and heat transfer characteristics on thermal performance inside the parallel flow channel with alternative ribs based on photovoltaic/thermal (PV/T) system. Applied Thermal Engineering, 185: 116237. https://doi.org/10.1016/j.applthermaleng.2020.116237

[7] Jalil, J.M., Ahmed, M.K., Idan, H.A. (2020). Experimental and numerical study of a new corrugated and packing solar collector. IOP Conference Series: Materials Science and Engineering, 765(1): 012026. https://doi.org/10.1088/1757-899X/765/1/012026

[8] Saadi, S., Benissaad, S., Poncet, S., Kabar, Y. (2018). Effective cooling of photovoltaic solar cells by inserting triangular ribs: A numerical study. International Journal of Energy and Environmental Engineering, 12(7): 488-494. https://doi.org/10.5281/zenodo.1317374

[9] Lei, C., Guo, D.X., Hua, S.W. (2016). Parametric study on thermal and hydraulic characteristics of laminar flow in microchannel heat sink with fan-shaped ribs on sidewalls - Part 1: Heat transfer. International Journal of Heat and Mass Transfer, 97: 1069-1080. https://doi.org/10.1016/j.ijheatmasstransfer.2016.02.077

[10] Lei, C., Guo, D.X., Hua, S.W. (2016). Parametric study on thermal and hydraulic characteristics of laminar flow in microchannel heat sink with fan-shaped ribs on sidewalls - Part 3: Performance evaluation. International Journal of Heat and Mass Transfer, 97: 1091-1101. https://doi.org/10.1016/j.ijheatmasstransfer.2016.02.075

[11] Ibtisam, A.H. (2018). Enhancement the performance of PV panel by using fins as heat sink. Engineering and Technology Journal, 36: 798-805. http://doi.org/10.30684/etj.36.7A.13

[12] Yong, L., Feng, S., Gongnan, X., Jiang, Q. (2018). Improved thermal performance of cooling channels with truncated ribs for a scramjet combustor fueled by endothermic hydrocarbon. Applied Thermal Engineering, 142: 695-708. https://doi.org/10.1016/j.applthermaleng.2018.07.055

[13] Shalaby, S.M., Elfakharany, M.K., Moharram, B.M., Abosheiasha H.F. (2022). Experimental study on the performance of PV with water cooling. Energy Reports, 8: 957-961. https://doi.org/10.1016/j.egyr.2021.11.155

[14] Mah, C.Y., Lim, B.H., Wong, C.W., Tan, M.H., Chong, K.K., Lai, A.C. (2019). Investigating the performance improvement of a photovoltaic system in a tropical climate using water cooling method. Energy Procedia, 159: 78-83. https://doi.org/10.1016/j.egypro.2018.12.022

[15] Guilherme, Z., Anderson, L.S., Osiris, C.J. (2018). Hybrid photovoltaic module for efficiency improvement through an automatic water cooling system: A prototype case study. Journal of Cleaner Production, 196: 535-546. https://doi.org/10.1016/j.jclepro.2018.06.065

[16] Chong, K.K., Tan, W.C. (2012). Study of automotive radiator cooling system for dense-array concentration photovoltaic system. Solar Energy, 86(9): 2632-2643. https://doi.org/10.1016/j.solener.2012.05.033

[17] Saeed, S.C.G. (2021). Solar photovoltaic cells performance improvement by cooling technology: An overall review. International Journal of Hydrogen Energy, 46(18): 10939-10972. https://doi.org/10.1016/j.ijhydene.2020.12.164

[18] Zubeer, S.A., Mohammed, H.A., Ilkan, M. (2017). A review of photovoltaic cells cooling techniques. E3S Web of Conferences, 22: 00205. https://doi.org/10.1051/e3sconf/20172200205

[19] Hussein, N.F., Ismaeel, A.A., Ibrahim, A.K. (2020). Influence of detergents types and clean method on PV cells performance: An experimental study. IOP Conferences Series: Materials Science and Engineering, 863(1): 012057. https://doi.org/10.1088/1757-899X/863/1/012057

[20] Watcharodom, N., Puangsombut, W., Khedari, J., Vatcharasatien, N., Hirunlabh, J. (2014). Experimental investigation of thermoelectric power generation using radiative heat exchange. Advanced Materials Research, 1025-1026: 1125-1133. https://doi.org/10.4028/www.scientific.net/AMR.1025-1026.1125

[21] Pisut, T., Preeda, C., Joseph, K. (2024). Improved performance of a radiative-based thermoelectric power generator with vertical finned absorber: An experimental investigation. International Journal of Heat and Technology, 42(1): 353-357. https://doi.org/10.18280/ijht.420138

[22] Idan, H.A., Kadhom, H.K., Faraj, S.R. (2024). Performance enhancement of PV panels by a channel shaped heat exchanger with an electromechanical control. Engineering and Technology Journal, 42(7): 818-832. https://doi.org/10.30684/etj.2024.143283.1575

[23] Gomaa, M.R., Mustafa, R.J., Rezk, H., Al-Dhaifallah, M., Al-Salaymeh, A. (2018). Sizing methodology of a multi-mirror solar concentrated hybrid PV/thermal system. Energies, 11(12): 3276. https://doi.org/10.3390/en11123276

[24] Hjerrild, N.E., Mesgari, S., Crisostomo, F., Scott, J.A., Amal, R., Taylor, R.A. (2016). Hybrid PV/T enhancement using selectively absorbing Ag–SiO2/carbon nanofluids. Solar Energy Materials and Solar Cells, 147: 281-287. https://doi.org/10.1016/j.solmat.2015.12.010

[25] Baranwal, N.K., Singhal, M.K. (2021). Modeling and simulation of a spiral type hybrid photovoltaic thermal (PV/T) water collector using ANSYS. In Advances in Clean Energy Technologies: Select Proceedings of ICET 2020. Springer, Singapore, pp. 127-139. https://doi.org/10.1007/978-981-16-0235-1_10

[26] Atkin, P., Farid, M.M. (2015). Improving the efficiency of photovoltaic cells using PCM infused graphite and aluminium fins. Solar Energy, 114: 217-228. https://doi.org/10.1016/j.solener.2015.01.037

[27] Abdelrazik, A.S., Al-Sulaiman, F.A., Saidur, R., Ben-Mansour, R. (2018). A review on recent development for the design and packaging of hybrid photovoltaic/thermal (PV/T) solar systems. Renewable and Sustainable Energy Reviews, 95: 110-129. https://doi.org/10.1016/j.rser.2018.07.013

[28] Rand, B.P., Genoe, J., Heremans, P., Poortmans, J. (2007). Solar cells utilizing small molecular weight organic semiconductors. Progress in Photovoltaics: Research and Applications, 15: 659-676. https://doi.org/10.1002/pip.788

[29] Al-Tahaineh, H., AlEssa, A.H. (2022). A hybrid TEG/evacuated tube solar collectors for electric power generation and space heating. Journal of Engineering and Applied Science, 69(1): 10. https://doi.org/10.1186/s44147-021-00065-1

[30] Syafiqah, Z., Amin, N.A.M., Irwan, Y.M., Majid, M.S. A., Aziz, N.A. (2017). Simulation study of air and water cooled photovoltaic panel using ANSYS. Journal of Physics: Conference Series, 908(1): 012074. https://doi.org/10.1088/1742-6596/908/1/012074